AIP Journal of Applied Physics

Temperature effects on the energy bandgap and conductivity effective masses of charge carriers in lead telluride from first-principles calculations

S. Venkatapathi, B. Dong, and C. Hin

Citation: Journal of Applied Physics **116**, 013708 (2014); doi: 10.1063/1.4887071
View online: http://dx.doi.org/10.1063/1.4887071
View Table of Contents: http://scitation.aip.org/content/aip/journal/jap/116/1?ver=pdfcov
Published by the AIP Publishing

Temperature effects on the energy bandgap and conductivity effective masses of charge carriers in lead telluride from first-principles calculations

S. Venkatapathi,[1,a)] B. Dong,[1,b)] and C. Hin[1,2,c)]
[1]Department of Mechanical Engineering, Virginia Tech, Blacksburg, Virginia 24061, USA
[2]Department of Materials Science and Engineering, Virginia Tech, Blacksburg, Virginia 24061, USA

(Received 1 April 2014; accepted 23 June 2014; published online 7 July 2014)

We determined the temperature effects on the electronic properties of lead telluride (PbTe) such as the energy bandgap and the effective masses of charge carriers by incorporating the structural changes of the material with temperature using ab-initio density functional theory (DFT) calculations. Though the first-principles DFT calculations are done at absolute zero temperatures, by incorporating the lattice thermal expansion and the distortion of Pb^{2+} ions from the equilibrium positions, we could determine the stable structural configuration of the PbTe system at different temperatures. © *2014 AIP Publishing LLC*. [http://dx.doi.org/10.1063/1.4887071]

I. INTRODUCTION

Thermoelectric materials employ the direct conversion of thermal to electrical energy, which plays an important role in various waste heat recovery applications.[1,2] Quantitatively, the thermoelectric efficiency of a material is characterized by a dimensionless parameter, figure of merit (zT), which is defined as $zT = \alpha^2\sigma T/(\kappa_{lat} + \kappa_{ele})$. The inter-related properties α, σ, κ_{lat}, κ_{ele}, and T are Seebeck coefficient, electrical conductivity, lattice thermal conductivity, electronic thermal conductivity, and absolute temperature, respectively. The higher a material's zT, the greater is the thermoelectric efficiency. The inter-related thermoelectric properties make it difficult to achieve high zT in materials.[1] Building nanostructured thermoelectric materials have proved to be an efficient method to enhance the zT.[3–7]

PbTe, a narrow direct bandgap semiconductor is a popular thermoelectric material in the temperature range from 300–850 K (Ref. 8) with unique properties such as low lattice thermal conductivity at high temperatures, increase in energy bandgap with temperature and strong temperature dependence of charge carrier scattering[9] and these properties favor lead telluride and its alloys as good thermoelectric materials.[10]

Significant advancements in various nanostructuring techniques have improved the zT of lead telluride based thermoelectric materials ranging from 1.5 at 773 K to 2.1 at 800 K.[11–13] Recently, zT of 2.2 at 915 K was achieved in a p-type PbTe-SrTe system by combining endotaxial nanostructuring and atomic scale substitutional doping.[14]

Many theoretical studies and calculations have been performed on PbTe and its alloys focusing on the electronic bandstructure and transport properties.[15–18] The strong temperature dependence of charge carrier effective mass is an important parameter that influences the electrical conductivity and the Seebeck coefficient of a material.[19] At finite temperatures, the band energies of a material differ from energy values obtained at zero temperature because of overall thermal expansion of the crystal and thermal motion of the ionic cores.[20] Because of these thermal effects, the finite temperature systems differ from the equilibrium frozen lattice approximation. Moreover, in our material of interest, PbTe, it was observed that the Pb mean square thermal displacements are significantly larger when compared to that of the Te displacements at elevated temperatures.[21]

In this study, we used first-principles calculations to determine the temperature dependence on the energy bandgap and electronic bandstructure of PbTe for an equivalent temperature range from 0–400 K. Although all the calculations were performed at 0 K, we introduced the temperature dependence by using the structural variations due to the finite temperature effects through lattice thermal expansion and displacement of ionic cores. The vibrational entropy of the system, which exists at finite temperatures, was neglected in our calculations since the density functional theory (DFT) calculations were performed at absolute zero temperature.

II. METHODOLOGY

The first-principles DFT calculations for the structural and electronic properties were performed using the Vienna ab initio simulation package (VASP)[22,23] program together with projector augmented wave (PAW) potentials[24] with a plane-wave basis set limited by the cutoff energy of 400 eV. All calculations were done using the generalized gradient approximation (GGA) developed by Perdew and Wang[25] for the exchange and correlation potential. A $12 \times 12 \times 12$ Monkhorst Pack[26] k-point mesh together with a Methfessel-Paxton[27] smearing of 0.1 eV was employed for the Brillouin zone integration. The effect of spin orbit interaction was included in the system along with the periodic boundary condition.

The equilibrium lattice parameter of PbTe at different temperatures from first-principles study[28] and experimental results on the thermal displacements of Pb^{2+} ionic cores from the equilibrium sites[9] were incorporated in our calculations. As the temperature increases, both Pb^{2+} and Te^{2-} ions will displace from their equilibrium lattice sites. To simplify

a)Electronic mail: saran@vt.edu.
b)Electronic mail: bind89@vt.edu.
c)Electronic mail: celhin@vt.edu.

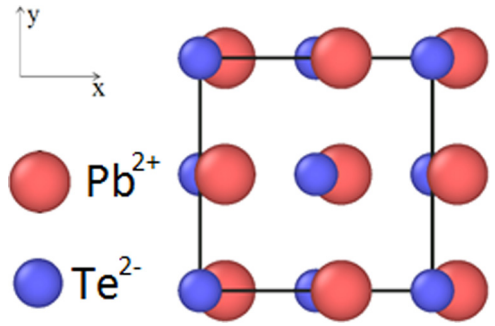

FIG. 1. Top view of PbTe crystal structure with Pb^{2+} ionic distortions in ⟨100⟩ direction at 300 K using OVITO software program.[29]

the thermal displacements of two different types of ions, we developed a model that defines the displacement of Pb^{2+} ions relative to the Te^{2-} ions by taking the later as the reference. From the previous results,[9,21] it is reasonable to take Te^{2-} ions as the reference because they are relatively more stable when compared to the Pb^{2+} ions.

The displacements were incremented in steps in all three directions and the atoms in the crystal structure were fully relaxed to find the stable configuration of the PbTe system at different temperatures. Fig. 1 shows the lattice displacement of Pb^{2+} ions at an equivalent temperature of 300 K in ⟨100⟩ direction.

III. RESULTS AND DISCUSSION

The final lattice off-centering of Pb^{2+} ionic cores from their equilibrium sites are shown in Table I. The distortions are predominant in the x direction, small along y and negligible along the z directions. In addition, as the temperature increases, the displacements along x increases, while those along y decreases. Since the displacements along z are negligible, the lattice distortions of the Pb^{2+} ionic cores are more likely to appear in the ⟨100⟩ direction as the temperature increases, especially when the temperature is above 200 K. Also, with the increase in temperature, the lattice distortions of Pb^{2+} ions tend to saturate.

The bond distance between Pb and Te atoms changes. At 0 K, with no displacements, the Pb-Te bond distance is 3.278 Å and at 400 K, the longest Pb-Te bond distance is 3.437 Å and the shortest is 3.155 Å.

Experimentally, it is observed that the energy bandgap of PbTe is temperature dependent.[20,30,31] The energy bandgap increases linearly with temperature until 400 K and above 400 K, it remains constant.[19]

TABLE I. Final displacements of Pb^{2+} ions at different temperatures in the stable crystal configuration.

	Calculated displacements of Pb^{2+} ions in Å		
Temperature in K	x	y	z
0	0	0	0
100	0.058	0.058	0.013
200	0.125	0.024	0.000
300	0.135	0.022	0.000
400	0.141	0.002	0.002

TABLE II. Temperature vs. energy bandgap in PbTe.

Temperature in K	Ref. bandgap in eV[19]	Calc. bandgap in eV
0	0.19	0.13
100	0.23	0.195
200	0.274	0.262
300	0.316	0.328
400	0.358	0.334

The reference energy bandgap values[19] and our calculated values are compared in Table II. The experimental linear temperature dependence of energy bandgap up to 400 K is given by Eq. (1)[19,20]

$$E_g = 0.19 + (0.42 \times 10^{-3})T, \quad T \leq 400\,\text{K}. \tag{1}$$

The linear regression of our calculated energy bandgap at different temperatures is given by Eq. (2)

$$E_g = 0.142 + (0.5 \times 10^{-3})T, \quad T \leq 400\,\text{K}. \tag{2}$$

The experimental data for the energy bandgap and our calculated values from each stable configuration are compared. As shown in Fig. 2, our theoretical calculations and experimental findings[20] are in relative agreement. However, we could see that the bandgap of PbTe is underestimated when compared to experimental results in the temperature range of concern because of the discontinuity in the exchange and correlation potentials used in our DFT calculations.

Other properties of interest calculated in this study are the conductivity effective masses of electrons and holes. The temperature dependence of charge carrier effective masses in PbTe is well studied.[31–33] We determined the conductivity effective masses of holes and electrons from the electronic bandstructure calculations. The general assumption of parabolic energy bands does not hold for lead telluride. PbTe has a complex bandstructure, and the non–parabolicity of the conduction and valence bands have to be considered to determine the electronic properties of the material.[19] The complex band structure is the result of band interactions.[34] The curvature of the band edges is an important parameter because the rate of change of slope of bandstructure is the effective mass of the charge carrier, which is used in evaluating the

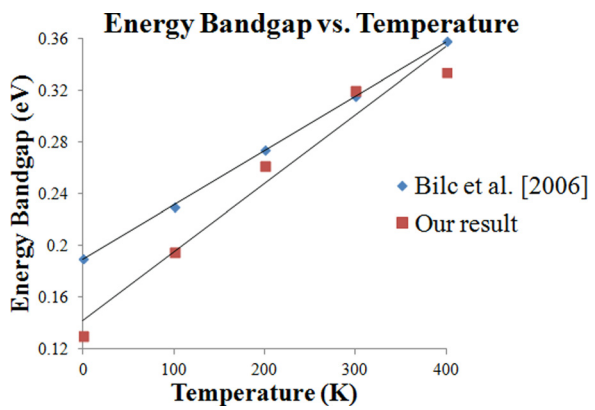

FIG. 2. Energy bandgap vs. temperature of PbTe.

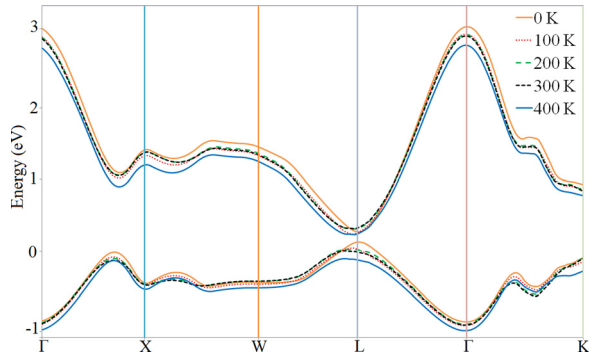

FIG. 3. Electronic band structure of PbTe at different temperatures representing the conduction and valence bands in the 1st Brillouin zone.

transport properties of the material. To incorporate this, we use the non–parabolic Kane's two-band model for the energy dispersion relation.[35] This model assumes that the band extrema for the conduction and the valence bands occur at the same k-point, which is the case in PbTe material, where the conduction and the valence bands occur at the L-point of the Brillouin zone.

The energy dispersion relation in terms of bandgap, conductivity effective mass, and wave vector is given by[36]

$$E(k) = \sqrt{\left(\frac{E_g}{2}\right)^2 + E_g \frac{\hbar^2 k^2}{2m^*}} - \frac{E_g}{2}. \quad (3)$$

The electronic bandstructure of the material has been calculated at different temperatures using the stable configurations of the system that was estimated previously for a temperature range from 0 to 400 K. The conduction and valence bands for the PbTe system determined from Pb^{2+} ionic displacements within the lattice expansion at different temperatures are represented in Fig. 3. Our primary area of focus is the band edges of the conduction and valence bands because the charge carriers in these energy levels primarily contribute to the transport properties of the material. We used the dispersion relation from Kane's two-band model[35] and did curve fitting with the band edges to obtain the conductivity effective masses of holes and electrons.

Curve fitting of the conduction and valence band edges at 300 K is shown in Fig. 4. Similar curve fittings were performed in this study for the temperature range, 0 and 400 K. We could see that away from the band edges, the dispersion relation is almost linear, which is typical for a narrow bandgap semiconductor. This is attributed to the semi

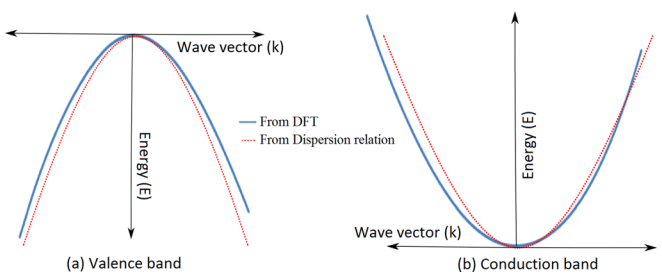

FIG. 4. Curve fitting the band edges of PbTe at 300 K using Kane dispersion relation. (a) Valence band and (b) conduction band.

TABLE III. Conductivity effective masses of charge carriers at different temperatures.

Temperature in K	Conductivity effective mass of holes m_h^*/m_0	Conductivity effective mass of electrons m_e^*/m_0
0	0.0635	0.0508
100	0.0704	0.0563
200	0.0782	0.0609
300	0.0824	0.0644
400	0.0894	0.0695

relativistic behavior of charge carriers in the electronic energy bands.[37]

The conductivity effective masses of holes and electrons in the 0–400 K temperature range calculated using the dispersion relation are shown in Table III. We also compare the conductivity effective masses of holes and electrons in the temperature range from 0–400 K with results from Wagner[38] and Landolt Bornstein[39] as shown in Fig. 5.

There is an increase in conductivity effective masses with temperature, which could also be interpreted from the band structure as shown in Fig. 3. The energy bands broaden and flatten leading to higher effective masses of charge carriers.

The relation between conductivity effective masses of charge carriers and temperature is expressed in Eqs. (4) and (5) as identified by Wagner[38]

$$\frac{m_h^*}{m_0} = 0.056 + (9 \times 10^{-5})T - (2 \times 10^{-8})T^2 \ , \quad (4)$$

$$\frac{m_e^*}{m_0} = 0.052 + (8 \times 10^{-5})T - (3 \times 10^{-8})T^2 . \quad (5)$$

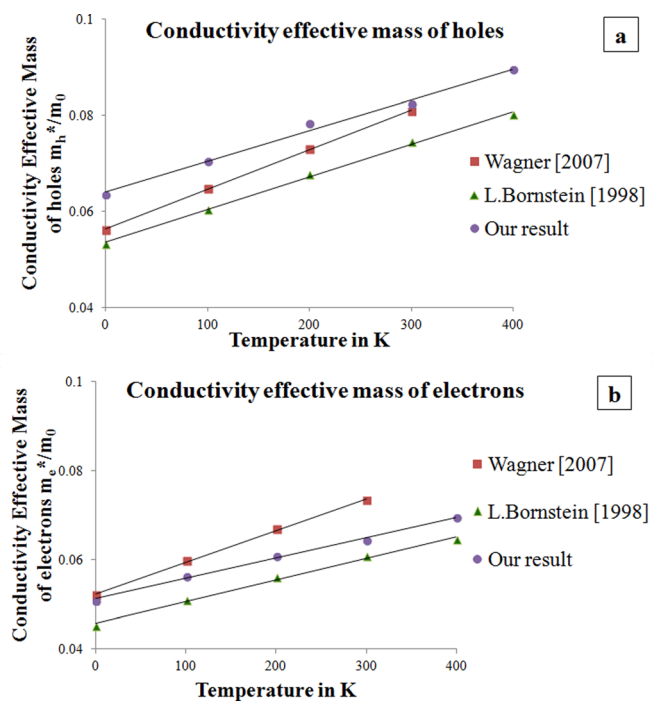

FIG. 5. Comparison of conductivity effective masses of (a) holes and (b) electrons in 0–400 K temperature range.

From our DFT calculations, we developed the relation between conductivity effective masses of charge carriers that are expressed in Eqs. (6) and (7)

$$\frac{m_h^*}{m_0} = 0.064 + (7 \times 10^{-5})T - (2 \times 10^{-8})T^2 \ , \qquad (6)$$

$$\frac{m_e^*}{m_0} = 0.051 + (5 \times 10^{-5})T - (1 \times 10^{-8})T^2 \ . \qquad (7)$$

IV. CONCLUDING REMARKS

From our DFT calculated results, the distortion of Pb^{2+} ionic cores has a direct relation with the enhancement of energy bandgap of PbTe with temperature. The displacement of Pb^{2+} ions saturates at approximately 450 K,[9] and the energy bandgap also increases linearly till 400 K and later remains constant. From the comparison of the band structure at different temperatures, we could see that the conduction and valence bands are highly non-parabolic and the increase in direct energy bandgap with temperature is clearly seen at the L point of the Brillouin zone.

The flattening of energy bands at the band edges with increase in temperature implies that the energy bands are becoming heavier. This leads to a higher effective mass of charge carriers that impacts the transport properties of a material. The electrical conductivity of a material will decrease because of reduction in mobility of charge carriers with large effective mass.[40] On the contrary, the Seebeck coefficient of a material increases with increase in the charge carrier effective mass.[40]

Though the first-principles DFT calculations are done at absolute zero temperatures, by incorporating the lattice thermal expansion and the distortion of Pb^{2+} ions from the equilibrium positions, we could determine the stable structural configuration of the PbTe system at different temperatures. Using the thermal lattice expansion and the distortion results, we could successfully determine the electronic properties of the materials at the desired temperature range. The linear temperature dependence of the energy bandgap and the effective masses of charge carriers were obtained from our first-principles calculations, which are important parameters in evaluating the transport properties of thermoelectric materials such as the Seebeck coefficient and electrical conductivity.

ACKNOWLEDGMENTS

The authors would like to acknowledge the financial support from Institute for Critical Technology and Applied Science (ICTAS) and the computational resources, technical support from Advanced Research Computing (ARC) at Virginia Tech. Also, the authors sincerely thank Dr. D. F. Cox, for the insightful discussions and suggestions.

[1]G. J. Snyder and E. S. Toberer, Nature Mater. **7**, 105 (2008).
[2]M. S. Dresselhaus, G. Chen, M. Y. Tang, R. G. Yang, H. Lee, D. Z. Wang, Z. F. Ren, J. P. Fleurial, and P. Gogna, Adv. Mater. **19**, 1043 (2007).
[3]B. Poudel, Q. Hao, Y. Ma, Y. C. Lan, A. Minnich, B. Yu, X. A. Yan, D. Z. Wang, A. Muto, D. Vashaee, X. Y. Chen, J. M. Liu, M. S. Dresselhaus, G. Chen, and Z. F. Ren, Science **320**, 634 (2008).
[4]G. Chen, M. S. Dresselhaus, G. Dresselhaus, J. P. Fleurial, and T. Caillat, Int. Mater. Rev. **48**, 45 (2003).
[5]K. Ahn, M. K. Han, J. Q. He, J. Androulakis, S. Ballikaya, C. Uher, V. P. Dravid, and M. G. Kanatzidis, J. Am. Chem. Soc. **132**, 5227 (2010).
[6]K. Biswas, J. He, Q. Zhang, G. Wang, C. Uher, V. P. Dravid, and M. G. Kanatzidis, Nat. Chem. **3**, 160 (2011).
[7]J. He, N. S. Girard, M. G. Kanatzidis, and V. P. Dravid, Adv. Funct. Mater. **20**, 764 (2010).
[8]D. J. Singh, Phys. Rev. B **81**, 195217 (2010).
[9]E. S. Božin, C. D. Malliakas, P. Souvatzis, T. Proffen, N. A. Spaldin, M. G. Kanatzidis, and S. J. L. Bilinge, Science **330**, 1660 (2010).
[10]B. A. Efimave, L. A. Kolomoets, Yu. I. Ravich, and T. S. Stavitskaya, Sov. Phys. Semicond. **4**, 1653 (1971).
[11]J. P. Heremans, V. Jovovic, E. S. Toberer, A. Saramat, K. Kurosaki, A. Charoenphakdee, S. Yamanaka, and G. J. Snyder, Science **321**, 554 (2008).
[12]Y. Pei, X. Shi, A. LaLonde, H. Wang, L. Chen, and G. J. Snyder, Nature **473**, 66 (2011).
[13]K. F. Hsu, S. Loo, F. Guo, W. Chen, J. S. Dyck, C. Uher, T. Hogan, E. K. Polychroniadis, and M. G. Kanatzidis, Science **303**, 818 (2004).
[14]K. Biswas, J. He, I. D. Blum, C. I. Wu, T. P. Hogan, D. N. Seidman, V. P. Dravid, and M. G. Kanatzidis, Nature **489**, 414 (2012).
[15]G. Martinez, M. Schluter, and M. L. Cohen, Phys. Rev. B **11**, 651 (1975).
[16]K. Hoang and S. D. Mahanti, Phys. Rev. B **78**, 085111 (2008).
[17]L. Zhang and D. J. Singh, Phys. Rev. B **81**, 245119 (2010).
[18]S. D. Mahanti and D. Bilc, J. Phys. Condens. Matter **16**, S5277 (2004).
[19]D. I. Bilc, S. D. Mahanti, and M. G. Kanatzidis, Phys. Rev. B **74**, 125202 (2006).
[20]Y. W. Tsang and M. L. Cohen, Phys. Rev. B **3**, 1254 (1971).
[21]C. Keffer, T. M. Hayes, and A. Bienenstock, Phys. Rev. Lett. **21**, 1676 (1968).
[22]G. Kresse and J. Furthmüller, Phys. Rev. B **54**, 11169 (1996).
[23]G. Kresse and J. Furthmüller, Comput. Mater. Sci. **6**, 15 (1996).
[24]G. Kresse and D. Joubert, Phys. Rev. B **59**, 1758 (1999).
[25]J. P. Perdew, in *Electronic Structure of Solids*, edited by P. Ziesche and H. Eschrig (Akademie Verlag, Berlin, 1991), Vol. 91, p. 11.
[26]H. J. Monkhorst and J. D. Pack, Phys. Rev. B **13**, 5188 (1976).
[27]M. Methfessel and A. T. Paxton, Phys. Rev. B **40**, 3616 (1989).
[28]Y. Zhang, X. Ke, C. Chen, J. Yang, and P. R. C. Kent, Phys. Rev. B **80**, 024304 (2009).
[29]A. Stukowski, Modell. Simul. Mater. Sci. Eng. **18**, 015012 (2010).
[30]R. N. Tauber, A. A. Machonis, and I. B. Cadoff, J. Appl. Phys. **37**, 4855 (1966).
[31]H. Yokoi, S. Takeyama, N. Miura, and G. Bauer, Phys. Rev. B **44**, 6519 (1991).
[32]H. A. Lyden, Phys. Rev. **135**, A514 (1964).
[33]A. K. Walton, T. S. Moss, and B. Ellis, Proc. Phys. Soc. **79**, 1065 (1962).
[34]M. Lundstrom, *Fundamentals of carrier transport* (Cambridge University Press, Cambridge, 2000).
[35]E. O. Kane, Semicond. Semimet. **1**, 75 (1966).
[36]E. O. Kane, J. Phys. Chem. Solids **1**, 249 (1957).
[37]W. Zawadzki, S. Klahn, and U. Merkt, Phys. Rev. Lett. **55**, 983 (1985).
[38]M. Wagner, "Simulation of thermoelectric devices," Ph.D. Dissertation, Vienna University of Technology (2007).
[39]Landolt-Börnstein, Group III Condens. Matter **41C**, 1 (1998).
[40]D. M. Rowe, Handbook of Thermoelectrics: Macro to Nano (CRC/ Taylor & Francis Group, Boca Raton, 2006).